Sensitivity analysis from single-well ERT simulations to image CO_2 migrations along wellbores

STEFANO PICOTTI [a], VIVIAN GRÜNHUT [b] , ANA OSELLA [b] , DAVIDE GEI [a] AND JOSÉ M. CARCIONE [a]

[a] Istituto Nazionale di Oceanografia e Geofisica Sperimentale – INOGS, Trieste, Italy
[b] Facultad de Ciencias Exactas y Naturales – Universidad de Buenos Aires, Argentina

Picotti, S., Grünhut, V., Osella, A., Gei, D., Carcione, J. M., 2013, *Sensitivity analysis from single-well ERT simulations to image CO_2 migrations along wellbores*, The Leading Edge 32(5), 504-512. DOI: 10.1190/tle32050504.1.

CO_2 plume imaging is a required step in CO_2 geological storage for both performance assessment and risk management purposes. This work has been performed in the frame of the CO2CARE project, whose aim is to develop tools and methodologies to monitor the CO_2 migration and verify the integrity of the wells in the long term after the site abandonment. Besides, the detection of any anomaly in due time is essential to perform a suitable remediation. For this purpose, downhole tools are permanently installed, but it is important to check the resolution and efficiency of the adopted techniques. In particular, this study investigates the possibility of using electrical resistivity tomography (ERT) to image CO_2 migrations around observation boreholes through a sensitivity study.

Under certain conditions, the ERT technique can image the subsurface distribution of electrical resistivity. Following the development of robust inversion algorithms and suitable data-acquisition systems, ERT has been applied to a wide range of environmental and engineering problems (Herman, 2001; Daily et al., 2004; Samouëlian et al., 2005; Martinelli et al., 2012). ERT applications are not constrained to surface investigations, because recent technical developments allow the use of downhole electrodes. Therefore, ERT may be appropriate for oil and gas reservoirs and deep saline aquifers characterization. The installation of electrodes deep in a reservoir can be done, cost effectively, during the completion of production/injection wells (Prevedel et al., 2008). The surveys can be performed in one-, two- or three-dimensions with different resolutions, from centimeters to hundred of meters. It is also worth noting an innovative method called LEMAM (Long Electrode Mise À La Masse) using the available metal-cased boreholes as very long electrodes distributing the current along the boreholes and measuring the electric field at the surface (Girard et al., 2009; Bourgeois and Girard, 2010).

ERT can be very important in CO_2 geological storage to monitor injected CO_2 migration as an alternative to/or in combination with seismic methods. Seismic methods has been proven to be very efficient in CO_2 geological storage monitoring. In saline aquifers, such as Sleipner and Nagaoka, repeated seismic surveys and time-lapse seismic data analysis allowed to map the CO_2 plume and its temporal and spatial evolution (Saito et al., 2006; Chadwick et al., 2010). However, this may not be the case elsewhere. For example, in some gas-depleted reservoirs, as the Rousse and K12-B gas fields (Vandeweijer et al., 2006), because of the large depths involved (4500 m and 3800 m respectively), CO_2 saturation variations can hardly be detected. Moreover, gas-depleted reservoirs may contain another gas, making the seismic response of the injected CO_2 small and easily masked by the noise (e.g., Picotti et al., 2012). This is also the case when trying to detect possible CO_2 migrations in the caprock, which may be due to faults and fractures or to damaged old wells. The difficulty here is that the host rock has a stiffer matrix and lower porosity and permeability than the reservoir formation. In addition, the CO_2 can be present in the supercritical state, with a density and a bulk modulus much higher than those of the gaseous phase (Picotti et al., 2012). The fluid effect under such conditions is smaller than that observed in a softer and more permeable rock, due to the reduced mobility of the fluid. Picotti et al. (2012) assessed the sensitivity of the reflection seismic method from surface for this specific problem, suggesting a reference detection threshold corresponding to a signal-to-noise ratio of about 10 dB. Another problem is the low sensitivity of the P-wave velocity to high saturations. In fact, when the CO_2 saturation exceeds 40 %, the variation of the velocity is weak and not enough to estimate the injected volume quantitatively if White's model of patchy saturation is used (Carcione and Picotti, 2006). Gassmann's theory is even more restrictive, with a threshold of 20% (e.g., Carcione et al., 2006).

In all these cases, complementary monitoring surveys, such as ERT or other methods based on electric or electromagnetic properties may be useful, since the electrical properties are more sensitive to the presence of fluids than the elastic properties (Ramirez et al., 1993; Carcione et al., 2007; Nakatsuka et al., 2009; Carcione et al., 2012). ERT in cross-well, single-well and surface-downhole configurations is an efficient

technique that can be employed to detect a gas within a conductive fluid and, more specifically, to image CO_2 plumes. Under certain conditions, it might be also helpful to detect small amounts of CO_2 near the wellbore. Hagrey et al. (2010) performed an ERT crosswell numerical study and showed that the method can discriminate the various components of a CO_2 storage in conductive saline reservoirs, namely, the plume, the host reservoir and the caprock. Recent studies (Christensen et al., 2006; Kiessling et al., 2010; Schmidt-Hattenberger et al., 2011; Bergmann et al., 2012) have shown the potential of ERT to detect resistivity changes caused by CO_2 injection and migration in geological reservoirs.
In particular, by using a surface-downhole configuration at Ketzin injection site, Bergmann et al. (2012) detected resistivity anomalies approximately 20 m above the reservoir, close to the observation wells. The authors suggest that these resistivity anomalies may be caused by weak coupling conditions of some electrodes to the formation, as a consequence of a possible infiltration of CO_2 in the uncemented part of the well annulus or CO_2 buoyancy-driven displacement of brine within the same well intervals (Bergmann et al. 2012). It is therefore reasonable to assume ERT as a potential tool to detect CO_2 migrations along wellbores. In order to estimate the amount of migrated CO_2 from downhole ERT measurements, the imaging technique can be very useful. If the CO_2 only invades the well annulus, it can be detected as shown by Bergmann et al. (2012). However, if for some reasons (e.g. cement degradation and fracturation of the caprock around the wells) the amount and extension of the migrated CO_2 is larger, it might also be imaged.
The aim of this work is to perform a sensitivity study with single-well simulations in order to show it is possible to image potential early-stage CO_2 migrations close to a well, above the reservoir. To perform our modelling on a realistic configuration, we benefit from the large and well documented case-history database of the CO2CARE project. We first design a synthetic model representing a possible CO_2 migration close to a well. This model, built on the basis of published data, represents a typical storage complex in a sandstone saline aquifer. Then, we perform numerical electrical resistivity forward modeling using different electrode configurations. Finally, we invert the resulting apparent resistivity models by ERT and compute the RMS difference between the original CO_2 migration model and the inverted resulting models.

Monitoring programs of the CO2CARE EU project

Important monitoring programs have been applied in several CO_2 storage pilot projects in the EU, using geophysical, geochemical and biological methods. The aim is to develop and validate tools and techniques to meet the requirements of the EU Directive on CCS (Carbon Capture and Storage) regarding geological storage safety and long-term integrity and stabilization. The results of these investigations revealed that CO_2 can be safely stored in deep saline aquifers and depleted hydrocarbon fields. The CO2CARE project aims to deliver technologies and procedures for abandonment and post-closure safety by addressing the research requirements of CO_2 storage site abandonment. One of the main objectives of the project is to suggest innovative plugging techniques to ensure long-term well integrity while studying feasible monitoring methods for early detection of CO_2 migrations. Dry runs for implementing closure scenarios at Sleipner, Ketzin and K12-B injection sites will be elaborated.
The Sleipner storage site is located in the Norwegian sector of the North Sea. This is the first commercial scale CCS project, which began in 1996 with the injection of the CO_2 separated from the extracted natural gas into a deep saline aquifer contained in the Utsira Sand formation, at approximately 1 km depth below the sea bottom (Chadwick et al., 2010). Since 1996 about 1 Mt CO_2 per year has been injected.
On the other hand, Ketzin pilot site is located near Postdam in a rural area with a few industrial infrastructures. The CO_2 storage reservoir is a saline aquifer, formed with fluvial deposit sandstones, located below an old natural gas storage reservoir. The CO_2 is trapped in an anticline structure of the German Basin, inside a sandstone unit of the Upper Triassic Stuttgart Formation, at 630–650 m depth. The injection began in June 2008 and after 39 months of operations about 53 thousand tonnes of CO_2 have been stored (Martens et al., 2012).
The K12-B storage site is located in the Dutch sector of the North Sea. The project started in 2004 when part of the CO_2 separated from the natural gas extracted from the K12-B reservoir was re-injected into the same reservoir located at about 3800 m depth below sea level (Vandeweijer et al., 2006). Since 2004 nearly 60 thousand tonnes of CO_2 has been injected.
In all these sites, the migration of the injected CO_2 is monitored at different scales, integrating together a broad range of geological, geophysical, geochemical and microbiological techniques. Field data sets are regularly acquired and used to update performance assessment models and scenarios, aiming at predicting the long term fate of CO_2. In practice, much work has been done in R&D projects, delivering valuable

information. On all these sites the monitoring campaigns have not shown any CO_2 migration outside the storage complex. We nevertheless aim at delivering monitoring tools and solutions for guarantying safe closure and post closure phases. Here, we design a representative scenario of a near-wellbore CO_2 migration to evaluate the ERT imaging technique sensitivity. Indeed, although the possibility of CO_2 migrations through the caprock along a wellbore is very low, it is one of the risks, and as such it has to be systematically considered in risk management and remediation studies. It has to be taken into account in monitoring plan designs, in agreement with the EU Directive recommendations on CCS.

Model of a possible CO_2 migration

In this work, we consider a typical storage scenario where the reservoir is a saline aquifer formed by fluvial deposit sandstones and the caprock consists in a thick mudstone layer. Since the main objective of this work is to optimize a permanent downhole ERT system to image possible CO_2 migrations very close to the wellbore, we focus our analysis on a maximum distance of 2 m from the wellbore casing. Moreover, our investigations address the transition zone between the sandstone reservoir and the caprock, where we assume that an array of electrodes can be installed outside the insulated casing, in contact with the formations. The previous CO2SINK project demonstrated that this is feasible. In fact, at the Ketzin injection site some of the wells are equipped with a Vertical Electrical Resistivity Array (VERA; Prevedel et al., 2008) to monitor the CO_2 plume by performing crosswell and surface-downhole investigations (Bergmann et al., 2012; Schmidt-Hattenberger et al., 2011; Kiessling et al., 2010).
As commonly observed at wellbores, we assume the presence of a thin layer of mud-cake between the casing and the formation, and a drilling mud invasion in the formation. Following the measurements of Wandrey et al. (2010), the thickness of the invaded zone in the reservoir should be less than 0.5 cm. Therefore, we assume the average thickness of the mud-cake and invaded zone to be 3 cm in the reservoir and 2 cm in the caprock (see Figure 1). The permeability may vary considerably along the radial direction due to the wellbore mud and formation damage while drilling. At the first 2 cm around the well, the permeability is very low (<1 mD, Wandrey et al., 2010) due to the presence of the mud-cake and drilling debris together with drilling mud in the pore space. However, we assume that the porosity ϕ, varies only 1 % radially. In the caprock mudstone ϕ = 12 % and in the reservoir sandstone ϕ = 30 % (Wandrey et al., 2010). The clay content (constant) is 50% in the caprock and 25% in the reservoir. Drilling-induced damages at the wellbore are frequently observed (using FMI measurements) and have been documented in the literature (e.g., Aadnoy and Bell, 1998). Practically, drilling operations may induce fractures and cracks in the rock surrounding a well, in a way that is not easily predictable, because it depends on many factors (e.g., depth, rock properties, fluids properties present in the pore space, including mud, and in situ stresses, pressure and temperature conditions). Generally, such fractures are supposed to extend within less than a 1m from the wellbore. Therefore, we make such an assumption to evaluate our ERT approach with this scenario, defining a caprock transition zone with drilling-induced fractures between 2 cm and 1 m from the metal casing, saturated only with brine, where CO_2 could migrate (see Figure 1). The formation is assumed to be intact at a distance greater than 1 m from the well.
In order to better detect potential CO_2 migrations, the resistivity of the drilling mud should be low. For this reason, oil-based drilling fluids are not recommended. Therefore, the drilling-mud resistivity is assumed to be 0.18 Ωm, which corresponds to a water-based mud with addition of a strong electrolyte to make it more conductive (Sherborne and Newton, 1942). The brine resistivity is 0.05 Ωm, while the formation resistivity without CO_2 is 1.5 Ωm in the mudstone and 0.46 Ωm in the reservoir (Kiessling et al., 2010). We use the complex refractive index method (CRIM) to obtain the missing parameters:

$$\rho = \left[(1-\phi)(1-C)\rho_q^{\gamma} + (1-\phi)C\rho_c^{\gamma} + \phi(1-S_g)\rho_b^{\gamma} + \phi S_g \rho_g^{\gamma}\right]^{1/\gamma}, \gamma = -1/2$$

(Carcione, 2007; Carcione et al., 2012), where C is the clay content, ϕ is the porosity, ρ is the resistivity of the formation, ρ_c, ρ_b, ρ_g are the clay, fluid and gas (CO_2) resistivities, respectively, and ρ_q represents the average grain (clastic) conductivity of the rock. Using the formation conductivity, we obtain ρ_q = 90.9 Ωm in the reservoir and 28.6 Ωm in the caprock. Then, using the CRIM equation and the drilling mud conductivity, we compute the conductivity of the invaded formations. The resistivity of the mud-cake

occupying the well annulus (the volume between the casing and the formation) is assumed to be the same of that corresponding to the invaded formation. All the properties are summarized in Tables 1 and 2.

Finally, we assume a possible CO_2 migration within the transition zone (2 cm - 1 m). The amount of migrated CO_2 is estimated to be about 150 kg, while the average CO_2 saturation is less than 10%. The CO_2 saturation in the reservoir is 30%. The CO_2 migration geometry is large at the base, and thin at the top, in order to study how the detection sensitivity is changing in relation to the thickness of the CO_2 migration. We use a grid composed by 200 x 5000 points, where the sample interval (grid spacing) is 1 cm. Figure 2 shows the gas saturation and resistivity models before and after the assumed CO_2 migration, where the well is located at the left side.
In this case we assume that the CO_2 cannot diffuse in the drilling mud invaded zone and in the mud-cake because of their very low permeability (<1 mD, Wandrey et al., 2010). However, the mud-cake might occupy only part of the well annulus, or it might not be present at all. In this case, the CO_2 may invade this zone occupied only by mud, producing CO_2 migrations with high CO_2 saturations. The resistivity value of the mud-cake in the well annulus (about 3.13 Ωm) is quite similar to the resistivity of a fluid mixture composed by mud and CO_2, where the CO_2 saturation is about S_g=70%. Therefore, this thin high-resistivity zone may also simulate a possible CO_2 migration in the well annulus, close to the well. We will also consider this case.

Electrical resistivity forward modeling

We simulate the geoelectric response of the CO_2 migration model of Figure 2 by using hypothetical arrays having different electrode configurations, i.e., Wenner-alpha, pole-pole and pole-dipole (see Figure 3a). These configurations are the most used in ERT (Reynolds, 1997). Moreover, for each configuration, different electrode spacings are tested. Note that the pole-dipole arrays have two parameters, the electrode spacing a and the dipole spacing factor n. The apparent resistivity distributions of both models (with and without the CO_2 migration) are computed by using the RES2MOD software (Loke, 2002), based on a finite-difference method in which the subsurface (in this case the medium outside the well) is discretized in a 2-D rectangular mesh, with a denser part in the area of interest. The values of the electrical resistivity in each cell are assigned accordingly to the model shown in Figure 2. Assuming the well electrically insulated, the interface where the electrodes are placed can be considered a dielectric medium. Gaussian random noise with 3 % amplitude is added to the apparent resistivity data in order to simulate a more realistic situation. Figure 3b shows the result of the forward modeling before and after the CO_2 migration using the pole-dipole configuration, where a = 1 m and n = 7. The CO_2 migration effect is clear in the apparent resistivity data distribution.
Bearing in mind that the purpose is to investigate the possibilities to image the CO_2 migration in an efficient way, we perform numerical simulations to find the highest a, i.e., the minimum number of electrodes, allowing the anomaly to be imaged. To do this, we varied a from 0.5 to 3 m, for all the considered electrode configurations.

Electrical resistivity tomography

Once we simulated the apparent resistivity data with random noise, we perform the inversion using the RES2DINV software (Loke, 2004), whose scheme is based on the least square method (Loke and Barker, 1996). Figure 4, 5 and 6 show, respectively, the ERT results obtained from the inversion of the simulated forward models before and after assuming the CO_2 migration with the three electrode configurations. We use 7 apparent resistivity levels, the electrode spacing a is 1 m and the number of electrodes is 55, covering all the profile. The CO_2 migration can clearly be imaged with all these electrode arrays when the dipole spacing factor n is set to 7, which is usually the maximum advisable for a real profile. In order to verify which configuration is the most effective, the RMS difference between the inverted and the original model is computed for each case. Figure 7 shows the progressive RMS difference obtained for each configuration as a function of the inversion iteration number. The RMS difference decreases as this number increases, and shows that the pole–dipole array has the smallest RMS error.
Increasing the electrode spacing, the CO_2 migration imaging becomes, as expected, more difficult. We find that, using an electrode spacing of 2.5 m and 22 electrodes to cover all the profile, the pole-dipole and the pole-pole arrays are not able to image the CO_2 migration. On the other hand, as shown in Figure 8a, the Wenner-alpha configuration can still identify (image) the CO_2 migration. Furthermore, we found that when

the electrode separation is larger than 3 m, the CO_2 migration cannot be imaged by any of these arrays. Otherwise, we verified that using all these configurations, the CO_2 migration becomes more visible by decreasing the electrode separation. In particular, Figure 8b shows that, decreasing the electrode spacing to 0.5 m, it is possible to image also the thin high-resistivity zone very close to the well, which is not visible in any of the previous experiments. Figure 8b shows the result obtained using the Wenner-alpha configuration; a very similar result can be obtained also using the pole-dipole configuration. In the previous simulations, this zone represents the mud-cake between the casing and the formation, and a thin zone of the formation invaded by the drilling mud, where the CO_2 cannot infiltrate. However, as explained in the model construction, if the mud-cake is not present this thin high-resistivity zone may also simulate a possible CO_2 migration in the well annulus, where the CO_2 saturation is S_g=70%. This simulation shows that to image possible CO_2 migrations in the well annulus, the electrode spacing has to be at most 0.5 m.

Conclusions

The electrical resistivity tomography (ERT) technique has been proven to be very efficient in CO_2 geological storage to monitor the injected plumes in cross-well and surface-downhole experiments. ERT acquisition design, in combination with seismic methods when possible, might be a very useful tool for imaging and quantification of CO_2 migrations.
In this work, we aim at testing the ERT technique to monitor possible early-stage CO_2 migrations along the wellbore at the caprock level, where seismic methods are less sensitive to the presence of the CO_2. To this aim, we built a representative model of a possible CO_2 migration close to a wellbore, on the basis of petrophysical data from sandstone saline aquifer reservoirs, and carried out single-well electrical simulations to perform a sensitivity study. In our scenario, we assumed that the CO_2 migration may occur within one meter around the well, because of the presence of fractures and cracks induced by drilling operations. We used different electrode spacings and three electrode configurations, i.e.: Wenner-alpha, pole-pole and pole-dipole. The ERT technique allows us to reconstruct the CO_2 migration by inverting the simulated forward apparent resistivity distributions. The RMS differences between the original CO_2 migration model and the inverted models suggest that the pole–dipole array is the most effective when the electrode spacing is lower than 2.5 m and the dipole spacing factor is 7. For larger electrode spacings, the Wenner-alpha configuration performs better, but the CO_2 migration can hardly be imaged. The inversions also suggest that possible CO_2 migrations in the well annulus can be imaged using the Wenner-alpha or the Pole-dipole configurations with electrodes spaced at most 0.5 m.

Acknowledgments

The research leading to these results has received funding from the European Union Seventh Framework Programme (FP7/2007-2013) under grant agreement n° 256625 (project CO2CARE), and from the industrial partners of the project. This work was also supported by the CO2MONITOR project. We would like to thank Jean-Pierre Deflandre and the GFZ staff for their constructive observations and suggestions.

References

Aadnoy, B.S. and Bell, J.S., 1998, Classification of drill-induce fractures and their relationship to insitu stress directions, Log Analyst, 39, 27-42.

Bergmann, P., Schmidt-Hattenberger, C., Kiessling, D., Rücker, C., Labitzke, T., Henninges, J., Baumann, G., Schütt, H., 2012, Surface-downhole electrical resistivity tomography applied to monitoring of CO_2 storage at Ketzin, Germany, Geophysics, 77, B253-B267.

Bourgeois, B., and Girard, J. F., 2010, First modelling results of the EM response of a CO_2 storage in the Paris basin, Oil & Gas Science and Technology – Rev. IFP, 65 (4), 597-614.

Carcione, J. M., 2007, Wave Fields in Real Media. Theory and numerical simulation of wave propagation in anisotropic, anelastic, porous and electromagnetic media, Elsevier. (Second edition, extended and revised).

Carcione, J. M., Gei, D., Picotti, S. and Michelini, A., 2012, Cross-hole electromagnetic and seismic modeling for CO2 detection and monitoring in a saline aquifer, Journal of Petroleum Science and Engineering, http://dx.doi.org/10.1016/j.petrol.2012.03.018.

Carcione, J. M., Ursin, B., and Nordskag, J. I., 2007, Cross-property relations between electrical conductivity and the seismic velocity of rocks, Geophysics, 72, E193-E204.

Carcione, J. M., and Picotti, S., 2006, P-wave seismic attenuation by slow-wave diffusion: Effects of inhomogeneous rock properties, Geophysics, 71, O1-O8.

Chadwick, R. A., Williams, G., Delepine, N., Clochard, V., Labat, K., Sturton, S., Buddensiek, M.-L., Dillen, M., Nickel, M., Lima, A. L., Arts, R., Neele, F., Rossi, G., 2010, Quantitative analysis of timelapse seismic monitoring data at the Sleipner CO_2 storage operation, The Leading Edge, 29, 170–177.

Christensen, N. B., Sherlock, D. and Dodds, K., 2006, Monitoring CO_2 injection with cross-hole electrical resistivity tomography, Exploration Geophysics, 37(1), 44–49.

Daily, W., Ramirez, A., Binley, A., and LaBrecque, D., 2004, Electrical resistance tomography, The Leading Edge, 23, 438-442.

Girard, J. F., Bourgeois, B., Rohmer, J., Schmidt-Hattenberger, C., 2009, The LEMAM array for CO2 injection monitoring: modelling results and baseline at Ketzin in August 2008, European Geosciences Union General Assembly (Vienna - Austria), Geophysical Research Abstracts, 11, EGU2009-7478-4.

Herman, R., 2001, An introduction to electrical resistivity in geophysics, American Journal of Physics, 69, 943-952.

Kiessling, D., Schmidt-Hattenberger, C., Schuett, H., Schilling, F., Krueger, K., Schoebel, B., Danckwardt, E., Kummerow, J., 2010, Geoelectrical methods for monitoring geological CO_2 storage: First results from cross-hole and surface-downhole measurements from the CO2SINK test site at Ketzin (Germany), International Journal of Greenhouse Gas Control, 4, 816-826.

Loke M. H., 2004, Tutorial: 2-D and 3-D electrical imaging surveys, course notes, http://www.geoelectrical.com/coursenotes.zip.
Loke, M. H., 2002, Rapid 2D resistivity forward modelling using the finite-diffrrence and finite-element methods, Geotomo Software, Malasia.

Loke, M. H. and Barker, R. D., 1996, Rapid least-squares inversion of apparent resistivity pseudosections by quasi-Nexton method, Geophysical Prospecting, 44, 131-152.

Martens, S., Kempka, T., Liebscher, A., Lüth, S., Möller, F., Myrttinen, A., Norden, B., Schmidt-Hattenberger, C., Zimmer, M., Kühn, M., 2012, Europe's longest-operating on-shore CO2 storage site at Ketzin, Germany: a progress report after three years of injection, Environmental Earth Sciences, 67 (2), 323-334, DOI: 10.1007/s12665-012-1672-5

Martinelli, H. P., Robledo, F. E., Osella, A. M., de la Vega, M., 2012, Assessment of the distortions caused by a pipe and an excavation in the electric and electromagnetic responses of a hydrocarbon-contaminated soil, J. Appl. Geophys, 77, 21-29, doi:10.1016/j.jappgeo.2011.10.016.

Nakatsuka, Y., Xue, Z., Yamada, Y., and Matsuoka, T., 2009, Experimental study on monitoring and quantifying of injected CO_2 from resistivity measurement in saline aquifer storage, Energy Procedia, 1, 2211–2218.

Picotti, S., Carcione, J. M., Gei, D., Rossi, G. and Santos, J. E., 2012, Seismic modeling to monitor CO_2 geological storage - The Atzbach-Schwanenstadt gas field, Journal of geophysical Research, 117, B06103, doi:10.1029/2011JB008540.

Prevedel, B., Wohlgemuth, L., Henninges, J., Krüger, K., Norden, B., and Förster, A., 2008, The CO2SINK boreholes for geological storage testing, scientific drilling, 6, 32-37, doi:10.2204/iodp.sd.6.04.2008.

Ramirez, A., Daily, W., LaBrecque, D., Owen, E., Chesnut, D., 1993, Monitoring an underground steam injection process using electrical resistance tomography, Water Resources Research, 29, pp 73-87.

Reynolds, J., 1997, An introduction to applied and environmental geophysics, John Wiley & Sons Ltd. Ed., 2nd Ed.

Saito, H., Azuma, H., Tanase, D., and Xue, Z., 2006, Time-Lapse crosswell seismic tomography for monitoring the pilot CO_2 injection into an onshore aquifer, Nagaoka, Japan, Exploration Geophysics, 37 (1), 30-36.

Samouëlian, A., Cousin, I., Tabbagh, A., Bruand, A., Richard, G., 2005, Electrical resistivity survey in soil science: A review, Soil & Tillage research, 83, 173-193.

Schmidt-Hattenberger, C., Bergmann, P., Kießling, D., Krüger, K., Rücker, C., Schütt, H. and Ketzin Group, 2011, Application of a Vertical Electrical Resistivity Array (VERA) for Monitoring CO2 Migration at the Ketzin Test Site: First Performance Evaluation, Energy Procedia, 4, 3363-3370.

Sherborne, J. E, and Newton, W. M., 1942, Factors Influencing Electrical Resistivity of Drilling Fluids, Transactions of the AIME, 146, 1, 204-220.

Vandeweijer, V. P., Van der Meer, L. G. H., Hofstee, C., D'Hoore, D., Mulders, F., 2006, CO_2 Storage and Enhanced Gas Recovery at K12-B, 71st Conference and Exhibition, Eur. Assoc. Geosci. Eng., Amsterdam.

Wandrey, M., Morozova, D., Zettlitzer, M., Würdemann, H., 2010, Assessing drilling mud and technical fluid contamination in rock core and brine samples intended for microbiological monitoring at the CO_2 storage site in Ketzin using fluorescent dye tracers, International Journal of Greenhouse Gas Control, 4, 972-980.

TABLES

Table 1 – Resistivity of the single constituents

Medium	Resistivity (Ωm)
Clay	5
Reservoir Grain	90.9
Caprock Grain	28.6
Drilling Mud	0.18
Brine	0.05
CO_2	∞

Table 2 – Formation properties.

Medium	Resistivity (Ωm)	Porosity (%)	Clay content (%)
Reservoir with mud (invaded zone) / mudcake	1.41	29	25
Reservoir saturated with brine	0.46	30	25
Reservoir saturated with brine and CO_2	0.88	30	25
Caprock with mud (invaded zone) / mudcake	3.13	11	50
Mud (30%) + CO_2 (70%)	3.13	100	0
Caprock with brine	1.50	12	50

FIGURE CAPTIONS

Figure 1 – Planar section (not in scale) of the well and the surrounding medium, where R_t = 98 cm and R_i = 2 cm in the mudstone, and R_t = 97 cm and R_i = 3 cm in the sandstone.

Figure 2 – Gas saturation (a) and resistivity (b) models before CO_2 migration. Gas saturation (c) and resistivity (d) models after CO_2 migration (damaged caprock scenario). The well is on the left side (black vertical line). The CO_2 saturation in the reservoir is 30%. The CO_2 migration scenario consists in a straight forward vertical CO_2 migration assumed within a one-meter caprock damaged zone.

Figure 3 – Representation of the electrode configurations (a) used in this work: Wenner-alpha, pole-dipole and pole-pole, where a is the electrode spacing, n is the dipole spacing factor and $d = na$. The current is injected through the outer electrodes and measured by the amperometer A, while the potential is measured between the inner electrodes by the voltmeter V. Results of the forward modeling before and after the CO_2 migration using the pole-dipole configuration (b), where a = 1 m and n = 7. It corresponds to the apparent resistivity of the medium, with 3% random noise added.

Figure 4 – Results of the ERT inversion before and after the CO_2 migration using the Wenner-alpha configuration, where a = 1 m.

Figure 5 – Results of the ERT inversion before and after the CO_2 migration using the pole-dipole configuration, where a = 1 m and n = 7.

Figure 6 – Results of the ERT inversion before and after the CO_2 migration using the pole-pole configuration, where a = 1 m.

Figure 7 – Plot of the RMS errors versus number of iterations, before and after the CO_2 migration, for the different electrode configurations, where a = 1 m and n = 7.

Figure 8 – Results of the ERT inversion before and after the CO_2 migration using the Wenner-alpha configuration, where the electrode spacing a is 2.5 m in (a), and 0.5 m in (b). Note that the thin high-resistivity zone very close to the well is visible.

FIGURES

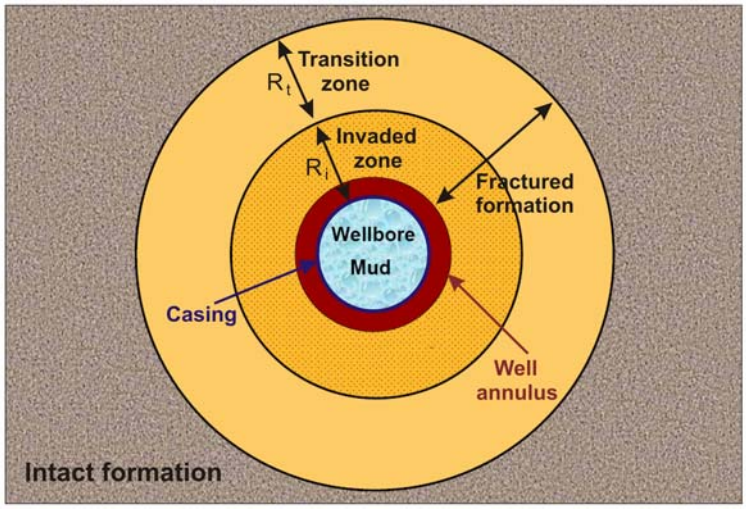

Figure 1

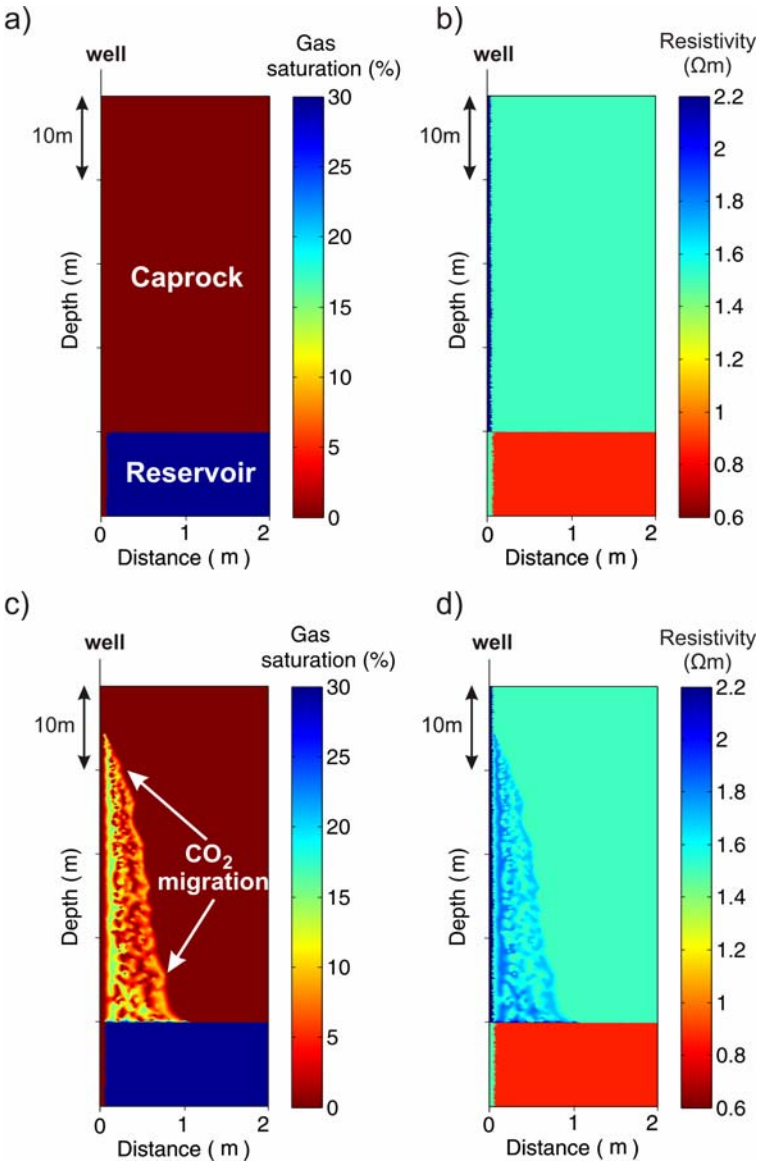

Figure 2

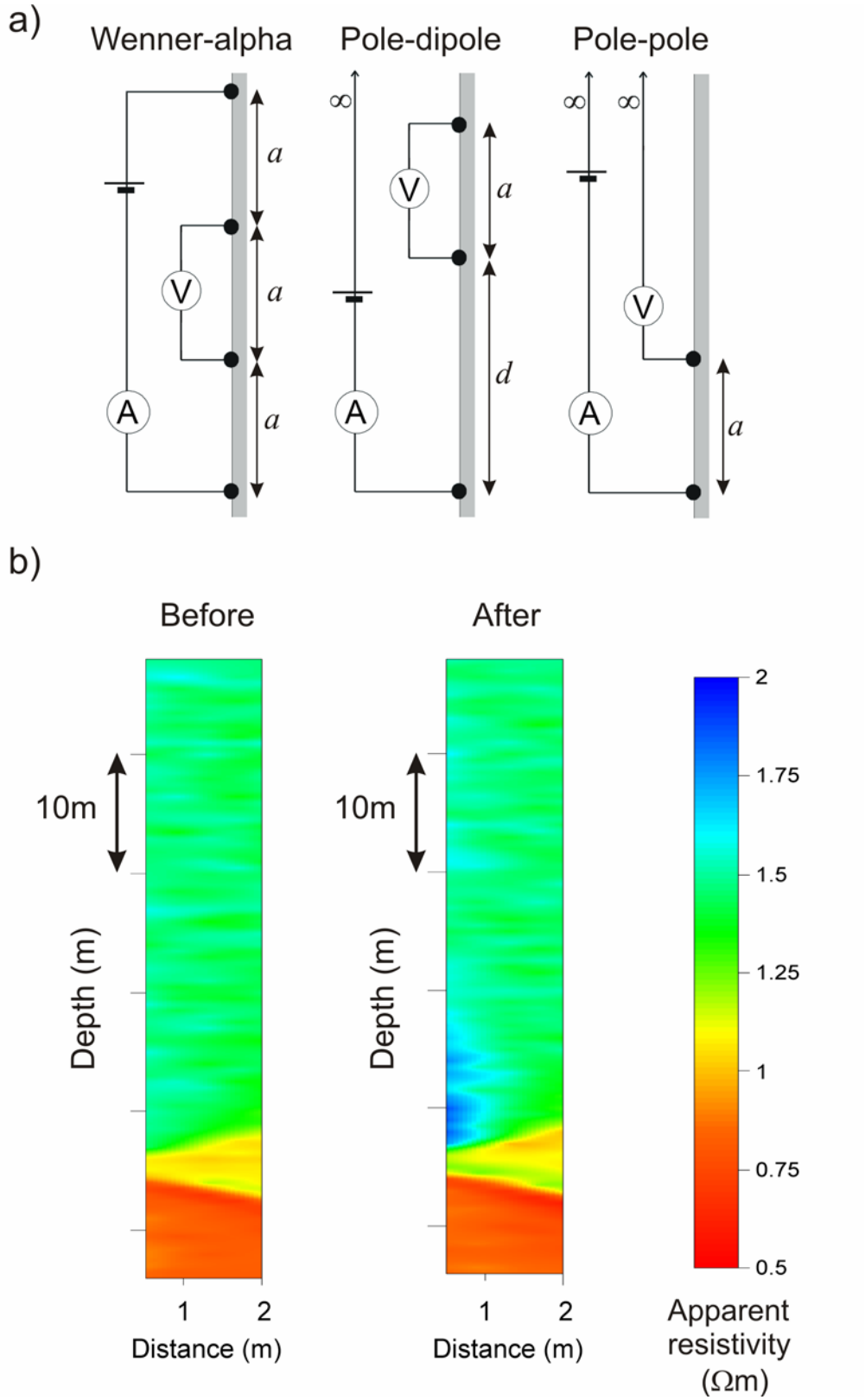
a)
Wenner-alpha
Pole-dipole
Pole-pole
a
a
a
V
A
∞
∞
∞
d
b)
Before
After
10m
10m
Depth (m)
Depth (m)
1
2
1
2
Distance (m)
Distance (m)
2
1.75
1.5
1.25
1
0.75
0.5
Apparent resistivity (Ωm)

Figure 3

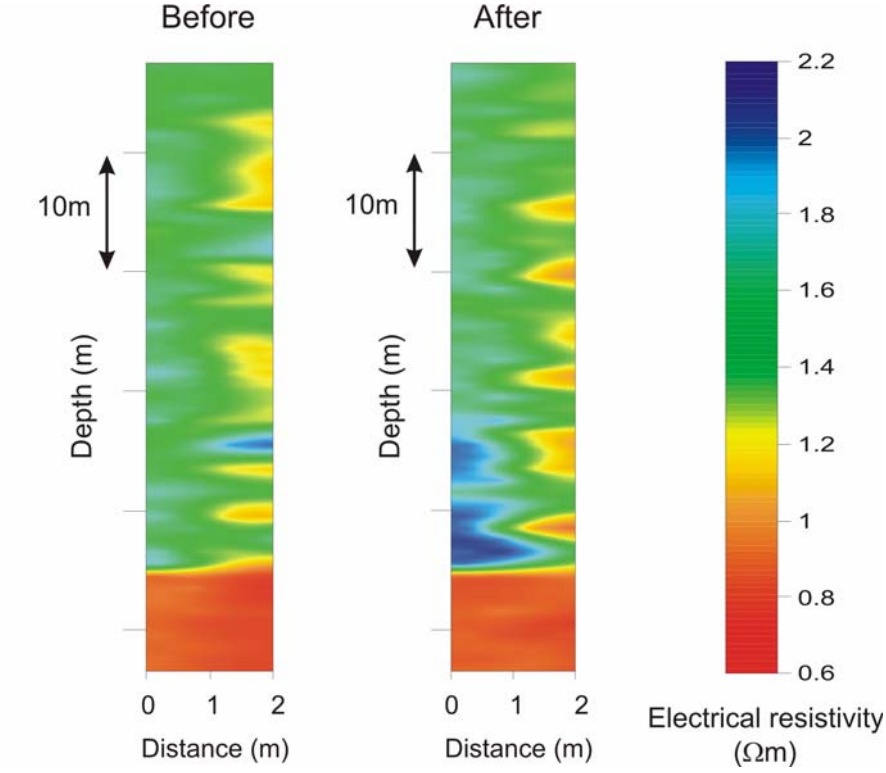

Figure 4

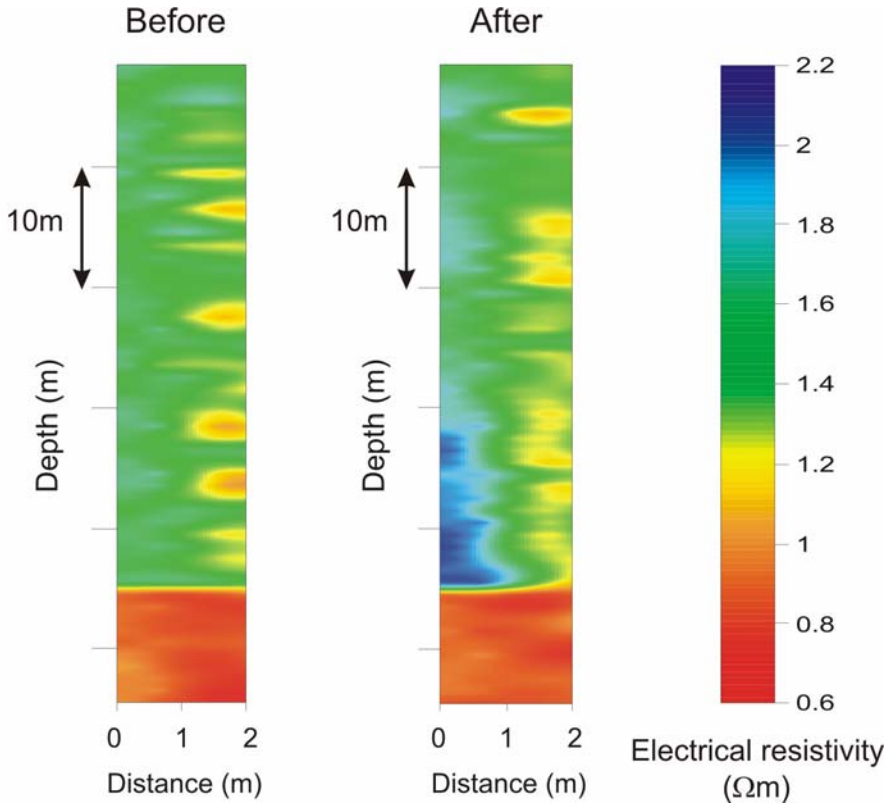

Figure 5

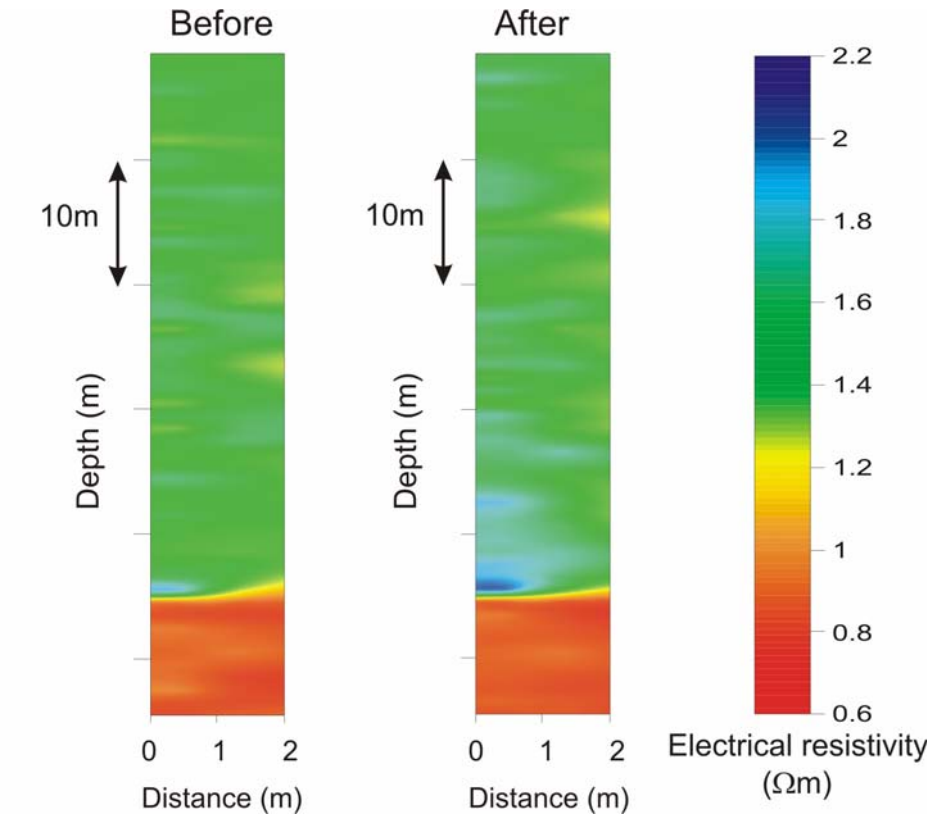

Figure 6

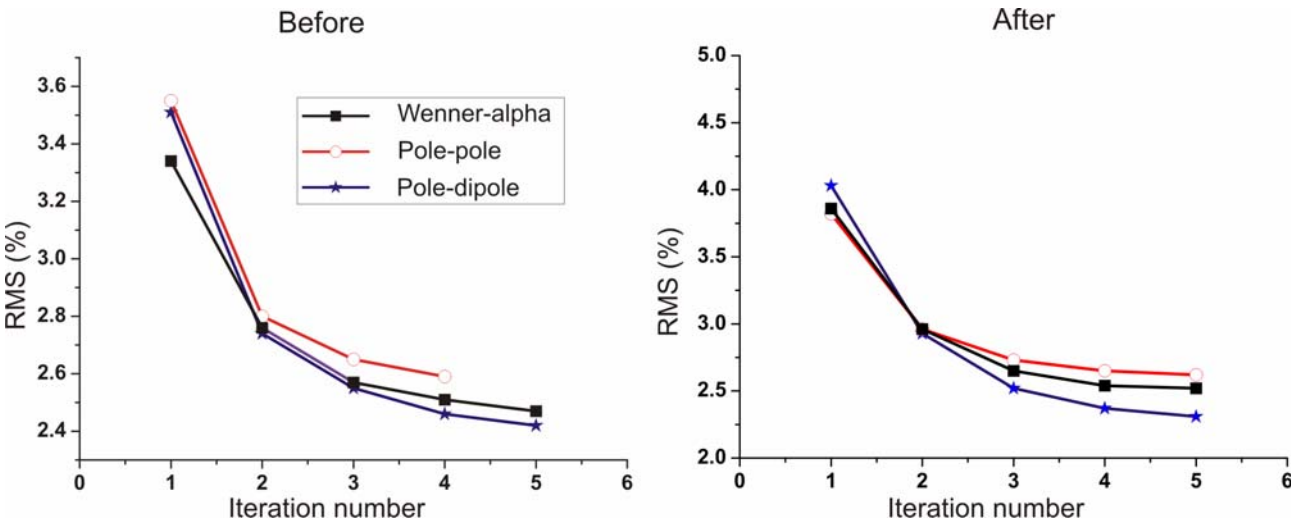

Figure 7

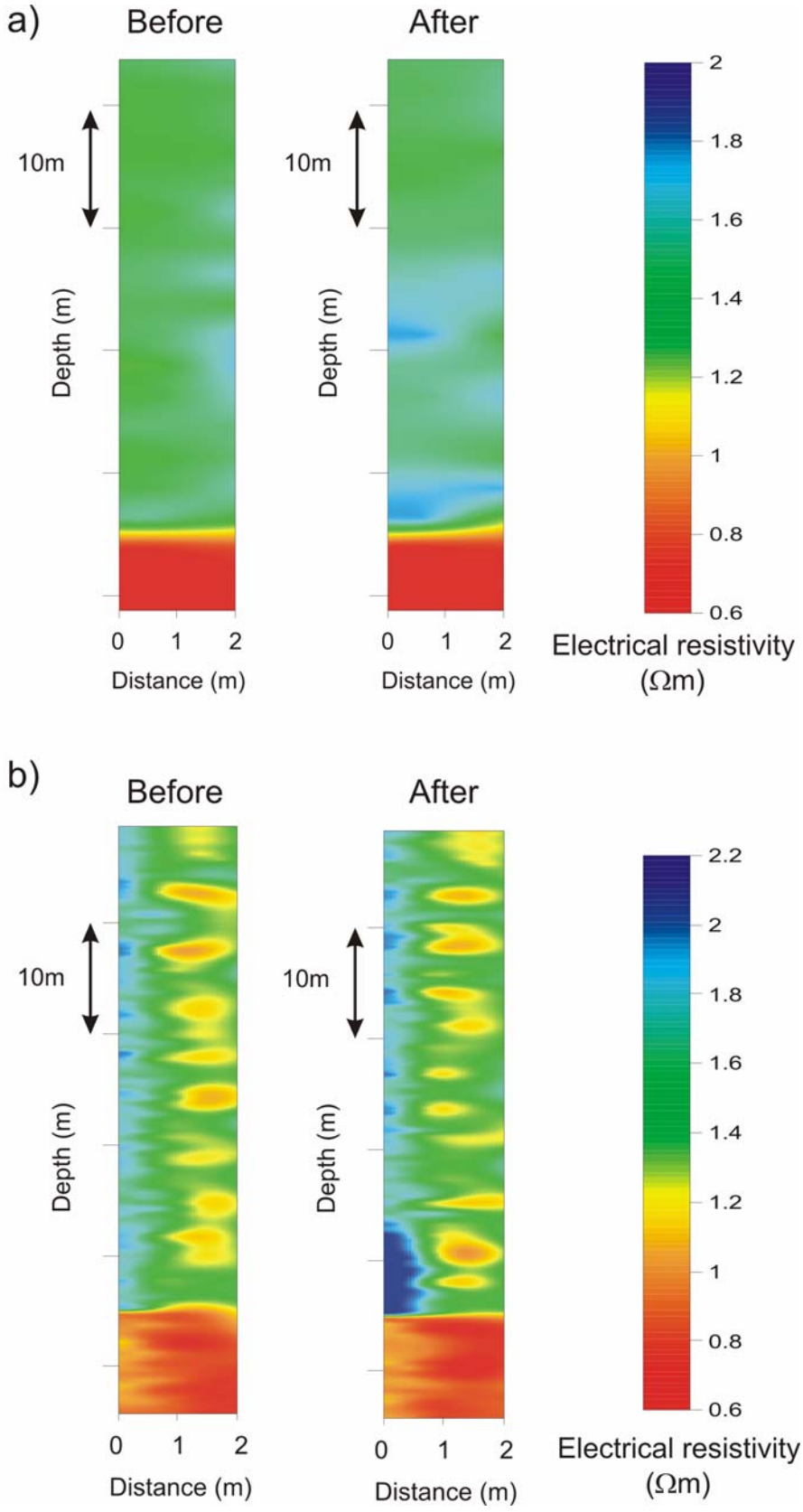
a)
Before
After
10m
Depth (m)
0
1
2
Distance (m)
2
1.8
1.6
1.4
1.2
1
0.8
0.6
Electrical resistivity
(Ωm)
b)
Before
After
10m
Depth (m)
0
1
2
Distance (m)
2.2
2
1.8
1.6
1.4
1.2
1
0.8
0.6
Electrical resistivity
(Ωm)

Figure 8